SPACE SCIENCES

Indigenous noble gases in the Moon's interior

Patrizia Will*, Henner Busemann, My E. I. Riebe, Colin Maden

The origin of volatiles in the Moon's interior is debated. Scenarios range from inheritance through a Moon-forming disk or "synestia" to late accretion by meteorites or comets. Noble gases are excellent tracers of volatile origins. We report analyses of all noble gases in paired, unbrecciated lunar mare basalts and show that magmatic glasses therein contain indigenous noble gases including solar-type He and Ne. Assimilation of solar wind (SW)–bearing regolith by the basaltic melt or SW implantation into the basalts is excluded on the basis of the petrological context of the samples, as well as the lack of SW and "excess ^{40}Ar" in the magmatic minerals. The absence of chondritic primordial He and Ne signatures excludes exogenous contamination. We thus conclude that the Moon inherited indigenous noble gases from Earth's mantle by the Moon-forming impact and propose storage in the incompatible element-enriched ("KREEP") reservoir.

INTRODUCTION

The widely accepted scenario for the origin of the Moon is the giant impact. Earlier models involved a moderately slow collision between proto-Earth and a Mars-sized impactor that expelled substantial amounts of material and produced a cloud of molten debris from which the Moon formed (*1*). More recent models invoke either a high-energy, hit-and-run scenario generating a much hotter debris disk (*2*), a giant impact onto a fast-spinning proto-Earth (*3*), the collision of a large impactor that gave rise to a circumterrestrial debris disk of molten and partially vaporized material from which the Moon rapidly accreted (*4*), or a cloud of mostly vaporized Earth and impactor material (a so-called "synestia") from which the Moon rapidly condensed (*5*). Very similar O isotopic signatures of Earth and Moon in contrast to distinct O isotopic compositions in other solar system bodies (*6*) imply either nearly complete mixing of Earth and an impactor (*7*), an impactor originating from a reservoir isotopically similar to Earth (*8*), or accretion of the Moon dominantly from terrestrial mantle material (*9*).

One consequence of the Moon's high-temperature formation is a depletion in volatile lithophile and volatile siderophile elements; the Moon was long considered substantially volatile-depleted relative to Earth (*10*). However, later discoveries of volatiles in lunar volcanic glasses (*11*), olivine-hosted melt inclusions (*12*), and apatite (*13*) suggest that highly volatile species were retained in the debris disk or synestia and accreted during the formation of the Moon (*12*, *14*). Similar deuterium over hydrogen (D/H) ratios of indigenous water in the Moon and in the terrestrial mantle indicate indeed only limited water loss, and D/H ratios are consistent with a chondritic origin of at least some water in the Earth-Moon system (*11*, *15*). Carbonaceous chondrites were proposed as the primary source of water, with possibly <20% contribution of cometary water (*16*). Consistently, the Xe heavy isotope composition in lunar anorthosites suggests possible admixture of cometary Xe (*17*). Chondritic water would have been inherited from a debris disk or synestia or delivered during the lunar magma ocean (LMO) phase, which may have lasted thousands to millions of years (*18*).

Noble gases are powerful tracers of the sources and processing of volatiles and can uniquely trace the volatiles during the formation of the Earth-Moon system. Similar to Earth, interior lunar volatiles would best be studied in mantle-derived samples such as the mare basalts that originate from partial melting of the deep mantle at depths of 200 to 400 km (*19*). However, lunar indigenous noble gases have not been detected so far [e.g., (*17*, *20*)].

Institute of Geochemistry and Petrology, ETH Zürich, Clausiusstrasse 25, 8092 Zürich, Switzerland.
*Corresponding author. Email: patrizia.w@mail.com

RESULTS

We analyzed interior fragments of the six Antarctic, paired (Supplementary Text), coarse-grained, and unbrecciated (*21*) lunar mare basalts LaPaz Icefield (LAP) 02205 (L05), 02224 (L24), 02226 (L26), 02436 (L36), 03632 (L32), and 04841 (L41) by noble gas mass spectrometry (Supplementary Text). These basalts have magmatic ages of ~3.0 billion years (Ga) [e.g., (*22*)]. They crystallized from an evolved, fractionated, low-Ti basaltic melt (Supplementary Text) (*23*) that was derived from an endogenously enriched source region with "KREEP" admixture (Supplementary Text) (*21*). The KREEP component accumulated incompatible elements such as K, rare earth elements (REE), and P, enriched during the latest stages of lunar mantle differentiation (*24*). Analyses of crystal size distributions suggest that the LAP mare basalts formed near the middle of a slowly cooled ~10-m-thick lava flow (*21*, *25*, *26*). The LAP meteorites (recovered mass of ~1.9 kg) were all ejected from the Moon together as one piece and spent ~35 thousand years in Moon-Earth transit (*27*).

Solar-type noble gases in the mare basalts

Two of six bulk interior fragments of the unbrecciated mare basalts, L24 and L36, have notably higher concentrations of ^{20}Ne (~100 to 1000 times higher), ^{36}Ar (~30 to 540 times higher), ^{84}Kr (~5 to 90 times higher), and ^{132}Xe (~2 to 20 times higher) than the other samples (tables S2 to S5). The isotopic compositions of these two samples are distinct from the other samples and indicate that they contain high amounts of trapped gases, in addition to the cosmogenic and radiogenic noble gases present in very similar amounts in all samples (Fig. 1 and figs. S1 to S3). Trapped noble gases can be, e.g., of chondritic or solar origin, or, in the case of Ar, Kr, and Xe, also due to atmospheric contamination. The Ne signature reveals trapped solar-type noble gases with a ^{20}Ne/^{22}Ne ratio of ~12.6, as determined by extrapolation through all bulk Ne data points (see Fig. 1A for a fit through these data points and the most solar-type noble gas–bearing glasses). Distinguishing between different trapped components is less straightforward in the other elements. The two solar Ne–bearing L24

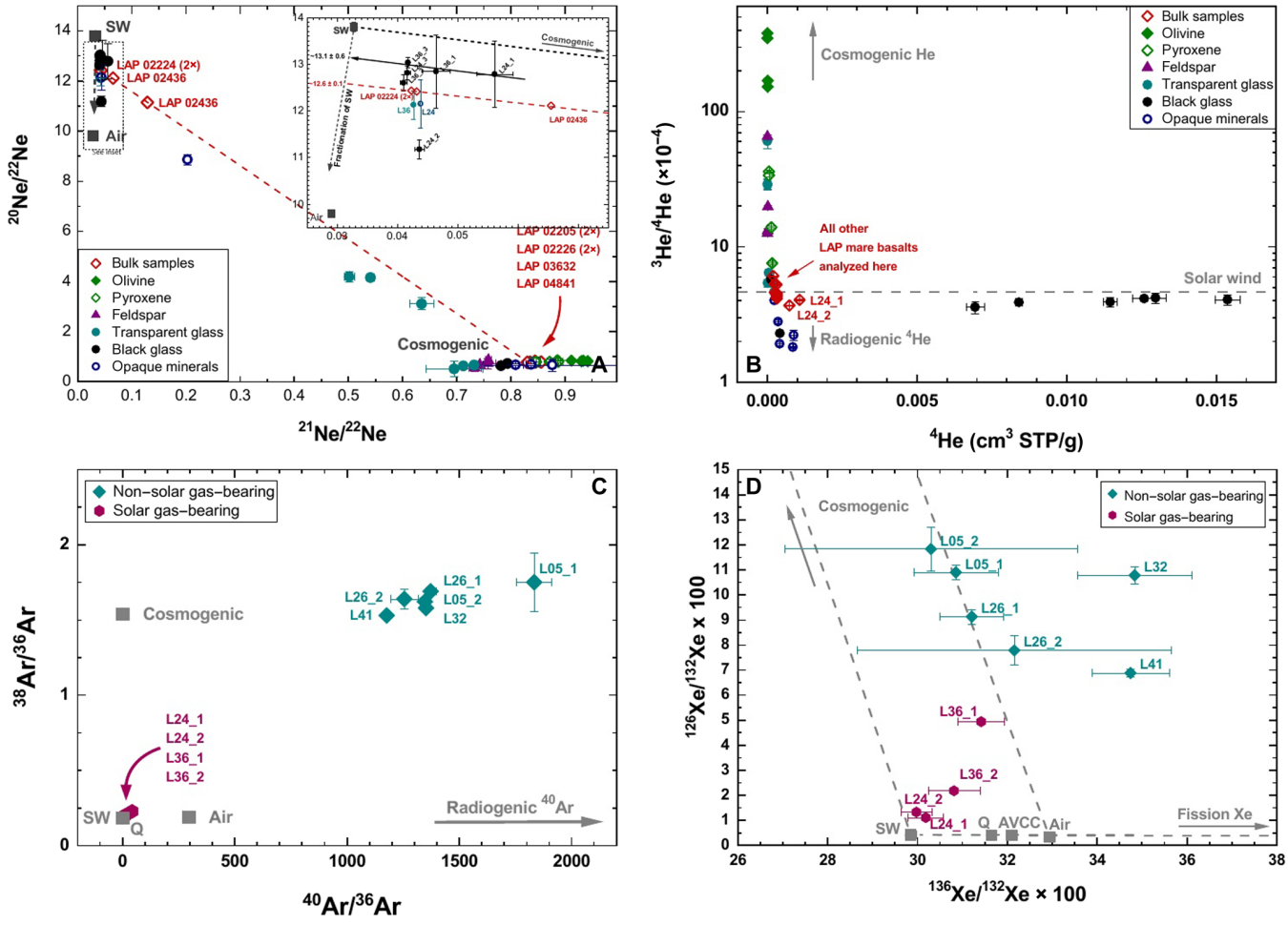

Fig. 1. Isotopic compositions of bulk samples, glasses, and mineral separates. (**A**) Neon three-isotope plot. L24 and L36 (two aliquots each) contain solar-type gases, dominantly Ne_{solar} with admixture of Ne_{cos}. L05 and L26 (two aliquots each) and L32 and L41 (one aliquot each) contain purely Ne_{cos}. Black glasses (L24 and L36) carry the solar-type gases. Some maskelynite and opaque grains were contaminated by solar gas–bearing black glass (fig. S5, A and B). Gray dashed arrow, calculated mass-dependent solar wind (SW) fractionation; red line, linear fit through bulk data points, $^{20}Ne/^{22}Ne_{solar} \sim 12.5$. Inset: Black dashed arrow, mass-dependent SW fractionation; black solid arrow, $^{20}Ne/^{22}Ne_{solar} \sim 13.1$ in black glass. (**B**) $^3He/^4He$ versus ^4He. Olivine, feldspar, and pyroxene have higher $^3He_{cos}$ production rates than the opaque minerals. The opaque minerals are dominated by $^4He_{rad}$. Solar-type He is dominant in black glass (L24 and L36), whereas black glass without dominant solar-type He shows similar $^3He/^4He$ as the opaque minerals due to additional $^4He_{rad}$; $^3He/^4He$ is similar to SW-He (fig. S1 for details). (**C**) $^{38}Ar/^{36}Ar$ versus $^{40}Ar/^{36}Ar$. All bulk samples contain similar concentrations of Ar_{cos} and $^{40}Ar_{rad}$ (tables S3 and S9). L24 and L36 are dominated by additional Ar_{solar}. Air-Ar is absent, consistent with He and Ne isotopes. (**D**) $^{126}Xe/^{132}Xe$ versus $^{136}Xe/^{132}Xe$ in bulk LAP basalts. Xenon in L24 is consistent with solar-type gases and fission Xe. A mixture of solar-type gases and Q, AVCC, air, or fission Xe is indicated for L36_2. L36_1 contains a higher Xe_{cos} concentration, while solar-type gases are not clearly indicated. Xenon in L05 and L26 is most likely air but could also be mixed SW and fission Xe. Admixture of fission Xe is visible in L32 and L41. References: SW (*33*, *69*), cosmogenic (*35*), air (*70*–*73*), Q (*28*), and AVCC (*29*, *30*). Error bars are mostly within symbols.

samples have the highest Xe concentrations and isotopic compositions most consistent with solar-type Xe (Fig. 1D), while the two L36 samples have Xe compositions that would also be consistent with chondritic gas, air, or a mixture of them with solar gases. The low concentrations of Kr and Xe in the bulk samples and, thus, large uncertainties on isotopic ratios prevent us from specifying details, including potential chondritic source components, e.g., so-called "*Q*" or "AVCC (average carbonaceous chondrite)" components (Fig. 1D and fig. S3) (*28*–*30*). Air is also possible based on the Kr isotopic composition alone, but this appears unlikely in light of the isotopic compositions of Ar and Xe. Having analyzed the bulk samples, it was hence clear that the LAP mare basalts contain a heterogeneously distributed, trapped noble gas component with a solar Ne signature, possibly a solar Xe signature, and trapped Ar and Kr, which could be solar or chondritic.

To identify the carrier of the trapped noble gases, we analyzed He and Ne in glass and mineral separates of feldspar, pyroxene, olivine, opaque minerals, transparent glass [likely dominantly maskelynite (Supplementary Text)], and black glass handpicked from the <100-μm-sized fractions of L05, L24, L26, and L36 (Supplementary Text). In the black glasses from L24 and L36, very high He and Ne concentrations of up to 1.5×10^{-2} cm^3 standard temperature and pressure (STP)/g of ^{4}He and 6.9×10^{-4} cm^3 STP/g of ^{20}Ne (table S7) were measured. He and Ne concentrations in the black glasses from L05 and L26 were considerably lower (e.g., 1.2×10^{-4} to 4.2×10^{-4} cm^3 STP/g of ^{4}He and 1.3×10^{-8} to 2.1×10^{-8} cm^3 STP/g of ^{20}Ne; table S7).

The $^{20}Ne/^{22}Ne$ ratios measured in black glasses from L24 and L36 ranged between 11.2 ± 0.2 and 13.0 ± 0.1 and are consistent with solar-type noble gases, which is also confirmed by $^{3}He/^{4}He$ ratios of 3.6×10^{-4} to 4.2×10^{-4} (table S7). A solar signature, albeit with highly variable and up to four orders of magnitude lower ^{20}Ne concentrations, was further detected in opaque minerals in L24 (0.0004×10^{-5} to 2.5×10^{-5} cm^3 STP/g of ^{20}Ne; table S7) and some transparent glasses (0.0001×10^{-4} to 0.9×10^{-4} cm^3 STP/g of ^{20}Ne; table S7) from L24, L26, and L36. The solar-type gases in the transparent glasses and opaque minerals likely originate from contamination by black glasses because (i) opaque minerals from the solar gas–bearing L36 lack solar noble gases and (ii) some transparent glasses from L24 and L36 contained black glass inclusions (Supplementary Text).

DISCUSSION

The solar ^{4}He concentrations in the black glasses (up to 1.5×10^{-2} cm^3 STP/g) are ~10 times lower than in Apollo/Luna soils (Fig. 2) (*31*), but ~3 times higher than in the most gas-rich terrestrial mantle samples [$\sim 10^{-5}$ cm^3 STP/g; "Popping Rock" (*32*)]. Similarly, the ^{20}Ne concentrations in the black glasses (up to 6.9×10^{-4} cm^3 STP/g) are approximately two orders of magnitude lower than in Apollo/Luna soils (up to $\sim 10^{-2}$ cm^3 STP/g ^{20}Ne) (*31*) and approximately four orders of magnitude higher than in the most gas-rich terrestrial mantle samples [$\sim 10^{-8}$ cm^3 STP/g; Popping Rock (*32*)]. The $^{4}He/^{20}Ne$ ratios of the black glasses range from 17.4 ± 1.0 to 32.3 ± 1.2 [table S7; uncorrected because cosmogenic (cos) and radiogenic (rad) contributions only marginally affect the data; Fig. 2] and are strongly fractionated compared to $^{4}He/^{20}Ne$ ratios of Apollo/Luna soils (typically ~50 to 60) (*31*) and solar wind (SW) (656 ± 5) (*33*). Hence, the solar-type noble gases in the black glasses are distinct from SW and the fractionated SW in lunar surface soil and regolith based on the elemental ratio and abundances.

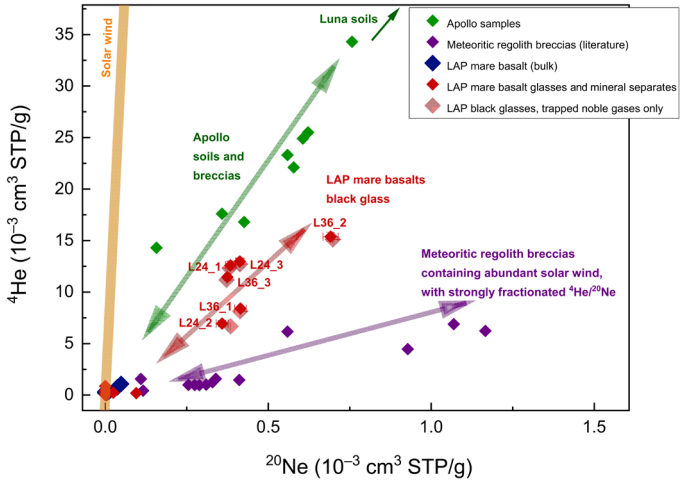

Fig. 2. ^{4}He versus ^{20}Ne plot. The solar-type noble gas–bearing black glasses (L24 and L36) show higher $^{4}He/^{20}Ne$ ratios (~17 to 32) than meteoritic regolith breccias (~4 to 20). SW ($^{4}He/^{20}Ne = 656 \pm 5$), Apollo/Luna soils, and breccias are given for comparison. The Apollo and Luna samples show higher ^{4}He concentrations (~15×10^{-3} to 35×10^{-3} cm^3 STP/g) than the meteoritic samples because they did not experience impact shock–induced ^{4}He loss (Supplementary Text), which all meteorites undergo inevitably to different degrees during the launching impacts. Error bars are mostly within symbols. Only the LAP black glasses from L24 and L36 are corrected for radiogenic ^{4}He and cosmogenic ^{4}He and ^{20}Ne (light red data illustrate the extent of correction, which only marginally shifts the data points because of the extremely high concentrations of solar noble gases). References: Meteoritic regolith samples (*37*), Apollo/Luna samples (*31*, *74*, *75*), and SW (*35*).

Cosmic ray exposure and source-crater pairing

Similar concentrations of cosmogenic noble gases are present in all six LAP basalts (table S9), and in all separates of feldspar, pyroxene, and olivine, the uncontaminated opaque mineral and transparent glass separates (samples with $^{20}Ne/^{22}Ne < 0.87$; table S7). The black glasses from L05 and L26 contain purely cosmogenic Ne, while He additionally includes $^{4}He_{rad}$ (table S7). On the basis of the similar cosmogenic concentrations and $(^{22}Ne/^{21}Ne)_{cos}$ ratios, the LAP basalts were exposed to cosmic rays for the same time in similar shielding conditions. The shallowest average shielding depth that the LAP basalts experienced is constrained, e.g., by the shielding depth indicator ratios $(^{131}Xe/^{126}Xe)_{cos} = 9.2 \pm 0.6$ (Supplementary Text) and $(^{78}Kr/^{83}Kr)_{cos} = 0.142 \pm 0.011$ (table S10), which imply a minimum average shielding depth of 140 g/cm^2 equaling ~0.5 m using the LAP mare basalt density of 3.0 g/cm^3 (*34*). The shielding depth might well have been higher, but surface residence for any extended time is excluded. The minimum average shielding depth and respective production rates (Supplementary Text) yield a minimum cosmic ray exposure (CRE) age of 63 ± 9 million years (Ma) based on $^{126}Xe_{cos}$ and 64 ± 5 Ma based on $^{78}Kr_{cos}$ and, accordingly, higher ages at larger depths (table S11). In any case, the similar CRE ages of all LAP basalts reveal that they experienced the same exposure history. Given their magmatic age of ~3 Ga [e.g., (*22*)], the LAP basalts were mostly shielded from cosmic rays [depth > 5 m (*35*)] in agreement with their origin from a depth of ~10 m within a lava flow proposed in (*25*). The basalts originated from the same shielding depth within a lava flow and were ejected as one rock by the same launching impact (source-crater pairing).

Absence of regolith-derived SW noble gases

The lunar regolith accumulates large amounts of SW that is implanted into the uppermost hundreds of nanometers of grain surfaces exposed to solar irradiation (*36*). Continued impacts shatter and stir the regolith, and, over time, most rock and mineral surfaces are randomly exposed to the SW. Thereby, the regolith acquires characteristic noble gas signatures: (i) very high SW concentrations of typically $\sim 10^{-1}$ to 10^{-2} cm^3 STP/g of ^{4}He and $\sim 10^{-3}$ to 10^{-4} cm^3 STP/g of ^{20}Ne (*31*, *37*), (ii) a SW isotopic signature (*36*), (iii) trapped $^{40}Ar/^{36}Ar$ ratios of ~1 to 10 due to incorporation of $^{36}Ar_{SW}$ and reimplantation of $^{40}Ar_{rad}$ degassing from the lunar surface ["excess ^{40}Ar" (*38*)], (iv) higher concentrations of cosmogenic noble gases than in underlying rock layers (e.g., mare basalts and anorthosites) due to generally decreasing production rates of cosmogenic noble gases with depth (*35*), and (v) distinct SW concentrations in different minerals due to mineral-specific trapping efficiencies, with especially the opaque minerals retaining high SW-He and SW-Ne concentrations (*36*).

The solar-type noble gas–bearing black glasses analyzed here lack all these characteristic regolith signatures:

1) All six LAP mare basalts have the same ^{40}Ar concentrations averaging to $2.5 \times 10^{-5} \pm 0.4 \times 10^{-5}$ cm^3 STP/g, while ^{36}Ar concentrations vary largely, depending on the presence of solar-type noble gases (0.15×10^{-7} to 99×10^{-7} cm^3 STP/g; table S3). Surface-derived solar gases would exhibit an excess ^{40}Ar signature as detailed above,

and the ^{40}Ar and $^{36}Ar_{SW}$ concentrations would be positively correlated (*38*). For instance, assuming a conservatively low $^{40}Ar_{excess}/^{36}Ar_{SW} = 1$ (*38*), the minimum expected $^{40}Ar_{excess}$ would be 9.9×10^{-6} cm^3 STP/g based on the $^{36}Ar_{solar}$ concentration in L24_1 (table S3). Adding the estimated $^{40}Ar_{rad}$ determined for this sample (Supplementary Text) gives a total ^{40}Ar concentration of ~3.5×10^{-5} cm^3 STP/g. This concentration is already ~28% higher than the measured ^{40}Ar concentration (table S3), which precludes excess ^{40}Ar. The very similar ^{40}Ar concentrations in the basalts do not allow for addition of regolith-derived $^{40}Ar_{excess}$. Shock-induced gas loss in the LAP basalts is negligible (*22*). Hence, regolith-derived $^{40}Ar_{excess}$ is absent. Notably, the above considerations are based on comparisons of the sample noble gas signatures and do not require an estimated mantle $^{40}Ar/^{36}Ar$, which is unknown and would depend on the magma source.

2) All six LAP meteorites have identical concentrations of cosmogenic noble gases regardless of the presence of solar-type noble gases (table S9). If regolith were admixed, then high and varying concentrations of cosmogenic noble gases accumulated during extended surface exposure would inevitably be associated (*36*), and the two solar gas–bearing LAPs would contain detectably higher cosmogenic noble gas concentrations (table S9).

Because the black glasses are the sole carrier of the solar-type noble gases, they would be the exclusive carrier of regolith-derived excess cosmogenic noble gases. The concentration of $^{20}Ne_{solar}$ is ~10 times higher in the black glasses than in the bulk samples, and we estimate that the black glasses make up ~10 weight % of the bulk rock. On the basis of these assumptions, we find that an additional ~5×10^{-12} cm^3 STP/g of $^{126}Xe_{cos}$ would be required in the black glasses to raise the $^{126}Xe_{cos}$ concentration of the bulk rock by clearly detectable 10%. This amount of $^{126}Xe_{cos}$ would be produced in a fresh basaltic regolith within ~12 Ma of surface exposure only. Hence, the lack of cosmogenic nuclide excesses in the LAP mare basalts supports that regolith contamination is absent.

3) Ilmenite, which is a major component in the opaque mineral separates, is most retentive for SW noble gases (*36*). However, solar-type gases are absent in opaque mineral separates from L36 and present only in a few opaque mineral separates of L24 (table S7). Therefore, we infer that the solar gas–bearing opaque mineral separates from L24 were contaminated by its solar gas–bearing black glass.

4) The noble gas concentrations of the solar gas–bearing black glasses are lower (~10^{-2} to 10^{-3} cm^3 STP/g of ^4He and ~10^{-4} cm^3 STP/g of ^{20}Ne; table S7) than in Apollo/Luna soils [~10^{-1} to 10^{-2} cm^3 STP/g of ^4He and ~10^{-3} to 10^{-4} cm^3 STP/g of ^{20}Ne (*31*)], and the elemental fractionation in $^4He/^{20}Ne$ is lower than commonly observed in regolith breccia meteorites, despite the comparatively high launch-induced shock level of the LAP meteorites [~60 GPa (*23*)]. High-energy launching impacts sufficient to eject lunar meteoroids to space cause severe flash heating and result in preferential diffusive loss of ^4He (Supplementary Text). Therefore, the $^4He/^{20}Ne$ ratios of regolith breccia meteorites are strongly fractionated (2.7 to 5.6) (*37*), while Apollo/Luna soils show $^4He/^{20}Ne$ ratios of ~38 to 110 (*31*). Black glasses in Apollo soil have a $^4He/^{20}Ne$ ratio of ~80 (*36*). The solar-type noble gases in the LAP black glasses thus have a unique composition, being more fractionated ($^4He/^{20}Ne \approx 20$ to 30) than SW in Apollo/Luna soils and black glasses but less fractionated than SW in regolith breccia meteorites.

5) The extrapolated $(^{20}Ne/^{22}Ne)_{solar}$ ratios in black glass reaching 13.1 ± 0.6 (Fig. 1A) and the $^3He/^4He$ ratios reaching 4.2×10^{-4} (table S7) in the LAP black glasses are closer to the isotopic composition of unfractionated SW [$^{20}Ne/^{22}Ne = 13.78 \pm 0.03$ and $^3He/^4He = 4.64 \times 10^{-4} \pm 0.09 \times 10^{-4}$ (*33*)] than typical Apollo/Luna soils (*31*). This excludes inheritance or admixture of regolith-derived SW to the black glasses.

6) The high concentrations of solar-type noble gases cannot be a result of trapping of regolith gases from the rock pore space, as the thin lunar exosphere with a very low pressure of ~10^{-15} bar would require too large pore space volumes. In addition, gases mobilized into the gas phase by diffusive loss induced by diurnal surface heating would lead to a favorable incorporation of the heavier noble gases Kr and Xe over He and Ne into the shock glass. This is not observed in the elemental noble gas ratios of the data.

The solar-type gases differ from regolith-derived SW. This is expected because the LAP mare basalts do not originate from a regolith breccia, but from a depth of 10 m within a lava flow (*25*), in which SW irradiation could not have occurred.

Indigenous solar-type noble gases from the Moon's interior

The lack of all characteristic regolith signatures, especially (i) the origin of the unbrecciated samples from within a thick lava flow, (ii) solar noble gas residence solely in the magmatic glasses without an accompanied regolith noble gas signature, and (iii) the magma source being a KREEP-rich reservoir strongly suggests that the solar-type noble gases in the LAP mare basalts were not acquired by assimilation of regolith material to the LAP melt nor accumulated during SW exposure in a lunar regolith. Thus, the solar-type noble gases must have been acquired by the LAP magma upon partial melting of a noble gas–bearing mantle reservoir, transported toward the surface by magma ascent, accumulated in residual melt batches of the lava flow because of their incompatibility in crystallizing phases (*39*), and trapped upon quenching of the magmatic melt. This is detailed in the following.

The LAP mare basalts contain two types of glasses: (i) shock glass veins and (ii) magmatic glasses. The shock glass veins are crosscutting the magmatic rocks and are formed from localized, shock-induced melting of the magmatic minerals (*21*, *23*). Because these minerals, mainly olivine, pyroxene, feldspar, and opaque minerals, are devoid of solar-type gases (Fig. 1A), they could not have delivered solar-type gases to the shock melt. We further observed no shock melt flow through the vein network. Instead, localized vein coloring represents the fully or partially molten adjacent minerals. Our observations coincide with those by Joy *et al.* (*23*), who showed that vein glass and the bulk rock material of the LAP samples have similar compositions and interpreted this to be the result of local melting. Therefore, no exterior melt was introduced into the LAP mare basalts, and shock vein glasses do not carry the solar-type noble gases.

The magmatic glass is present in mesostasis, i.e., the residual, incompatible element-enriched magmatic melt that partly crystallized and vitrified at the last stage of magma solidification. During melt crystallization, the incompatible volatiles are enriched in the residual liquid and trapped in the magmatic glasses upon quenching (*39*). The absence of the solar-type noble gases in four of the six LAP basalts reveals that the volatiles were inhomogeneously distributed over the residual melt batches. Inhomogeneous distribution of volatiles over mesostasis pockets is a common feature of lunar mare basalts (*40*). It results from exsolution of the late-stage residual melt into compositionally distinct conjugate liquids due to silicate-liquid immiscibility (*40*). The LAP basalts contain differentiated mesostasis

batches that formed from silicate-liquid unmixing (*23*). Noble gas solubility in melts strongly depends on the compositions and physical properties of the exsolved liquids. Less dense and more silica-rich liquids have the highest solubility for noble gases (*41*). The inhomogeneous distribution of the solar-type noble gases to the mesostasis pockets in the LAP basalts was likely caused by such compositional differences of the conjugate liquids (*40*) and hence noble gas solubility (*41*). The exact conditions under which the enormous enrichments of noble gases in the black glasses, particularly Ne with its solar isotopic signature, can be achieved, and whether the black glasses also contain large concentrations of other volatiles such as H, N, S, or halogens with potentially diagnostic isotope signatures (*11*–*13*), remain to be investigated in future experiments. We suggest that the solar-type noble gases trapped in the black glasses of L24 and L36 were liberated during partial melting of the deep lunar mantle from a hitherto undefined reservoir, then mixed into the LAP parental magma, delivered by magma ascent, and accumulated in the residual mesostasis melt during continued crystallization of the lava flow.

Reservoir of the solar-type noble gases in the lunar mantle

The absence of solar-type noble gases in previously analyzed mare basalts and gabbros (*42*, *43*) indicates either heterogeneous noble gas distribution in the lunar mantle or noble gas storage in a distinct reservoir not sampled before. The LAP basalts studied here are the first unbrecciated KREEP-bearing mare basalts (*44*) analyzed for noble gases. All other unbrecciated mare basalts and gabbros analyzed for noble gases so far (Asuka 881757, Yamato 793169, and NWA 032) do not contain a KREEP component (*45*–*47*) and lack solar-type noble gases (*42*, *43*).

D/H ratios consistent with a solar origin of the volatiles in KREEP were detected in KREEP-rich basaltic rocks (*48*). The δD values range from −380 to +790‰. The lowest values are closer to the protosolar δD value of −865 ± 32‰ [e.g., (*49*)] than to the δD range of +390 to +1100‰ observed in mare basalts [references in (*48*)]. The upper-limit δD value of the proto-Earth mantle has been estimated to be −218‰ (*50*), which is below the range of δD values in the mare basalts but coincides with the δD range in KREEP.

We suggest that the noble gases studied here support a common origin of the volatiles in Earth and Moon (*11*) and indicate storage of the lunar indigenous volatiles in a KREEP reservoir, which is consistent with the less clear-cut observations of H. The KREEP is considered to represent the residual melt fraction of the LMO that accumulated the incompatible elements (*51*). This includes the noble gases that are highly incompatible during fractional crystallization (*39*). We therefore conclude that the indigenous solar-type noble gases preserved in the LAP mare basalts are stored in a distinct KREEP or KREEP-rich reservoir in the lunar mantle. This reservoir underwent partial melting and was mixed with the LAP magma before or during ascent.

Incorporation of the solar-type noble gases into the Moon

We envision two scenarios that could account for the presence of solar-type noble gases in the Moon's interior. In the first scenario, the LMO that solidified up to a few millions of years after the Moon-forming event (*18*) could provide a time window for mixing impactor material into the lunar mantle. Carbonaceous chondrites and comets have N isotopic signatures and D/H ratios similar to the lunar mantle (*11*, *16*, *20*, *52*) and could have delivered volatiles including the noble gases to the LMO. In addition, enstatite and ordinary chondrites might have contributed water based on D/H ratios (*16*, *53*). Chondrites and comets contain abundant primordial noble gases with isotopic compositions that are decisively different from solar composition (*54*, *55*). The noble gas isotopic signatures of the lunar mantle reported in this study indicate that He and Ne are solar and not chondritic, while Ar, Kr, and Xe could be solar or chondritic. Contamination by chondritic impactors is unlikely due to the smooth chondrite-normalized platinum group element pattern (*21*), Re/Os and $^{187}Os/^{188}Os_{rad}$ ratios different from chondritic signatures (*56*), and variable, high Ni contents in troilite and FeNi metals with Ni-Co compositions different from those observed in chondritic, achondritic, and iron meteorites (*21*) in the LAP basalts that are consistently interpreted as magmatic signatures. On the basis of all the above, we thus exclude an exogenic origin of the observed solar He and Ne.

In the second scenario, the Moon accreted from a circumterrestrial debris disk or synestia, which contained terrestrial mantle and possibly impactor material ejected by the giant impact (*1*–*5*). Earth and Moon have indistinguishable isotopic compositions, for instance, in O (*6*), Si (*57*), Ti (*58*), and H [e.g., (*48*) and references therein]. The initial He isotopic composition of the terrestrial mantle is yet to be determined, Ne is solar (*59*), and Kr and Xe are likely chondritic [e.g., (*60*, *61*)]. The primordial light noble gases in the Moon detected in this study are similar to those in Earth's mantle. The solar-type $^{20}Ne/^{22}Ne$ ratios in the LAP mare basalts (Fig. 1A) coincide with solar-like $^{20}Ne/^{22}Ne$ ratios of ~13.0 ± 0.2 in terrestrial mantle plumes that likely sample deep mantle reservoirs possibly undisturbed since the formation of Earth (*62*, *63*). The heavy noble gases in the LAP basalts are less well constrained. While the L24 samples might rather point toward solar-type Xe than chondritic Xe, we do not have enough and sufficiently precise data to clearly distinguish between the two reservoirs, and the heavy noble gases could be similar to those in Earth's mantle. These observations show that the Moon could have inherited abundant solar-type noble gases and hence also other less volatile elements during the Moon-forming impact from Earth and not dominantly from an isotopically distinct impactor.

The isotopic composition of terrestrial mantle Ne has been used to argue for a mechanism to incorporate volatiles into Earth. If the $^{20}Ne/^{22}Ne$ ratio in Earth's interior is well below 13.0, then it was argued that dust exposed to SW early in the solar system accreted to form Earth, while if that ratio was well above 13.0, then trapping of nebula gas into a magma ocean could explain the origin of the volatiles [see, e.g., (*59*)]. The Ne data from the lunar interior in our study are consistent with both models. While Ne in the bulk samples suggests a $^{20}Ne/^{22}Ne$ ratio of 12.6 ± 0.1, supporting the former model, the black glass data (fit through the data points of L24_1, L36_1, and L36_3, as well as cosmogenic Ne in black glass, extrapolated to the solar Ne mass fractionation line) are also consistent with a high $^{20}Ne/^{22}Ne$ ratio of 13.1 ± 0.6, albeit with a large uncertainty. The $^{20}Ne/^{22}Ne$ ratios agree within uncertainties (see inset of Fig. 1A).

Experimental results show that our model of volatile storage in a KREEP-rich reservoir of the lunar mantle can account for the high amounts of volatiles observed in the black glass. Experimentally quenched glasses retained up to ~10^{-3} cm^3 STP/g of He and ~10^{-4} cm^3 STP/g of Ne at a pressure of 1 bar, while crystals grown from a melt of the same composition contained about four orders of magnitude lower noble gas concentrations (*39*). Hence, primordial volatiles from a KREEP-rich reservoir are a likely source for

enrichment of abundant indigenous noble gases in lunar magmatic glasses of mare basalts.

Indigenous noble gas concentrations in the Moon

The Moon appears more volatile rich than previously anticipated. The huge differences in noble gas concentrations between lunar and terrestrial samples discussed above and the isotopic compositions need to be explained by future geophysical models that seek to understand the formation of the Moon. Earth formed from accretion of solar nebula material. In a debris disk scenario of the Moon formation, volatile escape from the disk was limited to diffusion because of enrichment of heavy elements in the outer parts of the disk (*64*). Even the most volatile elements, including the noble gases, could be retained and accreted by the growing Moon. The fate of the highly volatile elements in a synestia scenario has not been studied so far, but the accretion of H was deemed possible (*5*). If so, then also heavier volatiles such as the noble gases could be retained in a synestia, available for accretion by the growing Moon.

Convection in the terrestrial mantle resulted in partial homogenization of the magma reservoirs, while in the Moon's mantle, reservoirs such as KREEP remained more isolated (*65*). Thus, an incompatible element-rich reservoir such as the KREEP, which likely strongly enriched the indigenous noble gases within the lunar mantle, could not develop and be preserved on Earth. Fractional crystallization of the LAP magma likely further enriched the indigenous noble gases in the residual melt batches. When the melts were quenched, the noble gas–rich magmatic glasses formed. The high concentration of indigenous noble gases in the KREEP-rich basalts is therefore not representative for the bulk lunar mantle but a consequence of these enrichment processes.

MATERIALS AND METHODS

Samples

We were allocated the sample splits LAP 02205,37 (hereafter L05), LAP 02224,10 (L24), LAP 02226,9 (L26), LAP 02436,8 (L36), LAP 03632,26 (L32), and LAP 04841,23 (L41) by the NASA Antarctic Meteorite Working Group (MWG) (table S1). All sample splits were taken from the interior parts of the meteorite, do not contain fusion crust, and hence very likely did not experience gas loss during entry into Earth's atmosphere. The MWG furthermore allocated the thin sections LAP 02205,36, LAP 02224,27, LAP02226,18, and LAP 02436,27.

Noble gas mass spectrometry

Bulk fusion He-Xe analyses

Sample splits of ~20 to 30 mg (table S1) wrapped in Al were extracted in one heating step to ~1700°C for 30 min and separated into three phases containing He-Ne, Ar, and Kr-Xe according to standard procedures (*66*). All stable He-Xe isotopes were analyzed in static vacuum using a custom-built, single-collector, magnetic-sector noble gas mass spectrometer equipped with Baur-Signer ion source (ETH Zürich). Ionization was induced at 100 eV of electron energy for analyses of L05, L24, L26, and L36 and at 45 eV for L32 and L41. The Kr-Xe phase typically contained ~6% of Ar, and the Ar phase typically contained ~1% of Kr and negligible Xe. Incomplete phase separation was corrected. Interferences contributed <1%, and no corrections were necessary. All details of the laboratory procedure are given in (*66*).

For blank correction, aluminum foils were measured the same way as the samples. Typical blank levels were 3.7×10^{-10} to 7.6×10^{-10} cm^3 STP in ^{4}He, 7.3×10^{-12} to 17×10^{-12} cm^3 STP in ^{20}Ne, 1.0×10^{-11} to 4.1×10^{-11} cm^3 STP in ^{36}Ar, 1.1×10^{-8} to 2.4×10^{-8} cm^3 STP in ^{40}Ar, 2.6×10^{-13} to 8.7×10^{-13} cm^3 STP in ^{84}Kr, and 0.6×10^{-13} to 2.4×10^{-13} cm^3 STP in ^{132}Xe and resulted in ≤2% blank correction for He-Ne, ≤1% correction for Ar for solar gas–rich samples and ≤10% for solar gas–free samples, and ≤4% correction for Kr-Xe for solar gas–rich samples and ≤45% for solar gas–free samples. Uncertainties given in this manuscript correspond to statistical errors at 1σ confidence level. For reference isotopes, the errors include uncertainties in determination of sample weights, blank correction, and sensitivities. Uncertainties in the isotopic ratios include statistical errors, uncertainties in mass discrimination, and blank correction.

Ultrahigh-sensitivity He-Ne analyses of the glass and mineral separates

To identify the carrier of the solar-type gases and to trace the origin of the solar signature in the Moon, six mineral and glass fractions with masses of 5 to 160 μg (table S6) containing olivine, pyroxene, feldspar, opaque minerals, and black and transparent (likely mostly maskelynite) glass were prepared for ultrahigh-sensitivity He-Ne analyses. The minerals and glasses were handpicked from <100-μm-sized fractions of L05, L24, L26, and L36 using a stereomicroscope [e.g., fig. S5 (A and B)], and mineralogical identification of each grain was done on the basis of optical properties. The transparent glasses were identified as maskelynite on the basis of (i) light microscopic observations on thin sections of these four LAP mare basalts that revealed full and partial maskelynization of feldspar as the only type of transparent glass present and (ii) nearly identical cosmogenic Ne isotopic compositions of the transparent glass and the feldspar, suggesting very similar chemical compositions (Fig. 1A). We observed contamination of maskelynite and opaque minerals by black glass that was most likely due to the mostly inseparable intergrowth of these phases. In all other cases, only microscopically pure grains were selected (see Supplementary Text).

The glass and mineral separates were degassed using a continuous-wave Nd:YAG Spectron SL902TQ laser emitting at 1064 nm with a maximal power of 65 W (=100%), and the beam width was limited to ~100 μm. The laser beam was directed onto the samples at 70% of the maximum emission power for 1 min. The gas purification procedure and further details of the laboratory routine are described in (*67*). He and Ne were analyzed using a unique, custom-built, ultrahigh-sensitivity, compressor-source noble gas mass spectrometer, which concentrates the sample gas into a miniaturized Baur-Signer–type ion source using an inverse Holweck-type molecular drag pump (*68*). Ionization was induced at an electron energy of 40 eV. Interferences contributed <1%, and no corrections were necessary. Total degassing of the samples was verified by occasional re-extractions at 80% of the maximum laser emission power, and the gases in these analyses were always below the detection limit.

At this mass spectrometer, we apply a unique measurement procedure. Background and memory of the laser chamber, gas extraction line, and mass spectrometer are monitored for typically five analytical cycles (~1700 s) in static vacuum before firing the laser for sample gas extraction. The sample gas released upon laser-induced heating then causes a step-like increase in the ion beam currents, and another six to seven analytical cycles are measured. The noble gas amounts are quantified by evaluating the "step size" of the beam currents at the time of gas extraction (*67*). Sensitivities and mass

discrimination are determined by frequent measurements of calibration gas with known gas amounts. Analytical blanks were determined by firing the laser at clean surfaces of the sample holder. The detection limits as determined from the blank levels plus two times the SDs of the blank measurements amounted to 1.0×10^{-15} to 1.5×10^{-15} cm^3 STP for ^{3}He and 8.6×10^{-16} to 8.8×10^{-16} cm^3 STP for ^{21}Ne and were higher for ^{4}He, ^{20}Ne, and ^{22}Ne.

SUPPLEMENTARY MATERIALS

Supplementary material for this article is available at https://science.org/doi/10.1126/sciadv.abl4920

REFERENCES AND NOTES

1. R. M. Canup, E. Asphaug, Origin of the Moon in a giant impact near the end of the Earth's formation. *Nature* **412**, 708–712 (2001).
2. E. Asphaug, C. B. Agnor, Q. Williams, Hit-and-run planetary collisions. *Nature* **439**, 155–160 (2006).
3. M. Ćuk, S. T. Stewart, Making the Moon from a fast-spinning Earth: A giant impact followed by resonant despinning. *Science* **338**, 1047–1052 (2012).
4. R. M. Canup, Forming a Moon with an Earth-like composition via a giant impact. *Science* **338**, 1052–1055 (2012).
5. S. J. Lock, S. T. Stewart, M. I. Petaev, Z. Leinhardt, M. T. Mace, S. B. Jacobsen, M. Ćuk, The origin of the Moon within a terrestrial synestia. *J. Geophys. Res. Planets* **123**, 910–951 (2018).
6. U. Wiechert, A. N. Halliday, D.-C. Lee, G. A. Snyder, L. A. Taylor, D. Rumble, Oxygen isotopes and the Moon-forming giant impact. *Science* **294**, 345–348 (2001).
7. R. C. Greenwood, J.-A. Barrat, M. F. Miller, M. Anand, N. Dauphas, I. A. Franchi, P. Sillard, N. A. Starkey, Oxygen isotopic evidence for accretion of Earth's water before a high-energy Moon-forming giant impact. *Sci. Adv.* **4**, eaao5928 (2018).
8. N. Dauphas, The isotopic nature of the Earth's accreting material through time. *Nature* **541**, 521–524 (2017).
9. N. Hosono, S.-I. Karato, J. Makino, T. R. Saitoh, Terrestrial magma ocean origin of the Moon. *Nat. Geosci.* **12**, 418–423 (2019).
10. K. Righter, Volatile element depletion of the Moon—The roles of precursors, post-impact disk dynamics, and core formation. *Sci. Adv.* **5**, eaau7658 (2019).
11. A. E. Saal, E. H. Hauri, J. A. Van Orman, M. J. Rutherford, Hydrogen isotopes in lunar volcanic glasses and melt inclusions reveal a carbonaceous chondrite heritage. *Science* **340**, 1317–1320 (2013).
12. A. E. Saal, E. H. Hauri, M. L. Cascio, J. A. Van Orman, M. C. Rutherford, R. F. Cooper, Volatile content of lunar volcanic glasses and the presence of water in the Moon's interior. *Nature* **454**, 192–195 (2008).
13. J. W. Boyce, Y. Liu, G. R. Rossman, Y. Guan, J. M. Eiler, E. M. Stolper, L. A. Taylor, Lunar apatite with terrestrial volatile abundances. *Nature* **466**, 466–469 (2010).
14. E. H. Hauri, T. Weinreich, A. E. Saal, M. C. Rutherford, J. A. Van Orman, High pre-eruptive water contents preserved in lunar melt inclusions. *Science* **333**, 213–215 (2011).
15. R. Tartèse, M. Anand, F. M. McCubbin, S. M. Elardo, C. K. Shearer, I. A. Franchi, Apatites in lunar KREEP basalts: The missing link to understanding the H isotope systematics of the Moon. *Geology* **42**, 363–366 (2014).
16. J. Barnes, D. A. Kring, R. Tartèse, I. A. Franchi, M. Anand, S. S. Russell, An asteroidal origin for water in the Moon. *Nat. Commun.* **7**, 11684 (2016).
17. D. V. Bekaert, G. Avice, B. Marty, B. Henderson, M. S. Gudipati, Stepwise heating of lunar anorthosites 60025, 60215, 65315 possibly reveals an indigenous noble gas component on the Moon. *Geochim. Cosmochim. Acta* **218**, 114–131 (2017).
18. L. T. Elkins-Tanton, S. Burgess, Q.-Z. Yin, The lunar magma ocean: Reconciling the solidification process with lunar petrology and geochronology. *Earth Planet. Sci. Lett.* **304**, 326–336 (2011).
19. S. R. Taylor, The moon, in *Encyclopedia of the Solar System*, L.-A. McFadden, P. R. Weissman, T. V. Johnson, Eds. (Academic Press, ed. 2, 2007), pp. 227–250.
20. E. Füri, P. H. Barry, L. A. Taylor, B. Marty, Indigenous nitrogen in the Moon: Constraints from coupled nitrogen-noble gas analyses of mare basalts. *Earth Planet. Sci. Lett.* **431**, 195–205 (2015).
21. M. Anand, L. A. Taylor, C. Floss, C. R. Neal, K. Terada, S. Tanikawa, Petrology and geochemistry of LaPaz Icefield 02205: A new unique low-Ti mare-basalt meteorite. *Geochim. Cosmochim. Acta* **70**, 246–264 (2006).
22. V. A. Fernandes, R. Burgess, A. Morris, ^{40}Ar-^{39}Ar age determinations of lunar basalt meteorites Asuka 881757, Yamato 793169, Miller Range 05035, La Paz Icefield 02205, Northwest Africa 479, and basaltic breccia Elephant Moraine 96008. *Meteorit. Planet. Sci.* **44**, 805–821 (2009).
23. K. H. Joy, I. A. Crawford, H. Downes, S. S. Russell, A. T. Kearsley, A petrological, mineralogical, and chemical analysis of the lunar mare basalt meteorite LaPaz Icefield 02205, 02224, and 02226. *Meteorit. Planet. Sci.* **41**, 1003–1025 (2006).
24. N. J. Hubbard, C. Meyer Jr., P. W. Gast, H. Wiesmann, The composition and derivation of Apollo 12 soils. *Earth Planet. Sci. Lett.* **10**, 341–350 (1971).
25. J. M. D. Day, L. A. Taylor, On the structure of mare basalt lava flows from textural analysis of the LaPaz Icefield and Northwest Africa 032 lunar meteorites. *Meteorit. Planet. Sci.* **42**, 3–17 (2007).
26. E. Hill, L. A. Taylor, C. Floss, Y. Liu, Lunar meteorite LaPaz Icefield 04841: Petrology, texture, and impact-shock effects of a low-Ti mare basalt. *Meteorit. Planet. Sci.* **44**, 87–94 (2009).
27. K. Nishiizumi, D. J. Hillegonds, K. C. Welten, Exposure and terrestrial histories of lunar meteorites LAP 02205/02224/02226/02436, MET 01210, and PCA 02007, in *Proceedings of the 37th Lunar and Planetary Science Conference* (Lunar and Planetary Institute, 2006), abstract 2369.
28. H. Busemann, H. Baur, R. Wieler, Primordial noble gases in "phase Q" in carbonaceous and ordinary chondrites studied by closed-system stepped etching. *Meteorit. Planet. Sci.* **35**, 949–973 (2000).
29. D. Krummenacher, C. M. Merrihue, R. O. Pepin, J. H. Reynolds, Meteoritic krypton and barium versus the general isotopic anomalies in meteoritic xenon. *Geochim. Cosmochim. Acta* **26**, 231–249 (1962).
30. O. Eugster, P. Eberhardt, J. Geiss, Krypton and xenon isotopic composition in three carbonaceous chondrites. *Earth Planet. Sci. Lett.* **3**, 249–257 (1967).
31. N. M. Curran, M. Nottingham, L. Alexander, I. A. Crawford, E. Füri, K. H. Joy, A database of noble gases in lunar samples in preparation for mass spectrometry on the Moon. *Planet. Space Sci.* **182**, 104823 (2020).
32. M. Moreira, J. Kunz, C. Allègre, Rare gas systematics in popping rock: Isotopic and elemental compositions in the upper mantle. *Science* **279**, 1178–1181 (1998).
33. V. S. Heber, R. Wieler, H. Baur, C. Olinger, T. A. Friedmann, D. S. Burnett, Noble gas composition of the solar wind as collected by the Genesis mission. *Geochim. Cosmochim. Acta* **73**, 7414–7432 (2009).
34. W. S. Kiefer, R. J. Macke, D. T. Britt, A. J. Irving, G. J. Consolmagno, The density and porosity of lunar rocks. *Geophys. Res. Lett.* **39**, L07201 (2012).
35. C. M. Hohenberg, K. Marti, F. A. Podosek, R. C. Reedy, J. R. Shirck, Comparisons between observed and predicted cosmogenic noble gases in lunar samples, in *Proceedings of the 9th Lunar and Planetary Science Conference* (Lunar and Planetary Institute, 1978), pp. 2311–2344.
36. P. Signer, H. Baur, U. Derksen, P. Etique, H. Funk, P. Horn, R. Wieler, Helium, neon, and argon records of lunar soil evolution, in *Proceedings of the 8th Lunar and Science Conference* (Lunar and Planetary Institute, 1977), pp. 3657–3683.
37. M. Mészáros, B. A. Hofmann, I. Leya, A noble gas data collection of lunar meteorites. *Meteorit. Planet. Sci.* **53**, 1104–1107 (2018).
38. O. Eugster, D. Terribilini, E. Polnau, J. Kramers, The antiquity indicator argon-40/argon-36 for lunar surface samples calibrated by uranium-235-xenon-136 dating. *Meteorit. Planet. Sci.* **36**, 1097–1115 (2001).
39. V. S. Heber, R. A. Brooker, S. P. Kelley, B. J. Wood, Crystal-melt partitioning of noble gases (helium, neon, argon, krypton, and xenon) for olivine and clinopyroxene. *Geochim. Cosmochim. Acta* **71**, 1041–1061 (2007).
40. J. F. Pernet-Fisher, G. H. Howarth, Y. Liu, Y. Chen, L. A. Taylor, Estimating the lunar mantle water budget from phosphates: Complications associated with silicate-liquid-immiscibility. *Geochim. Cosmochim. Acta* **144**, 326–341 (2014).
41. G. Lux, The behavior of noble gases in silicate liquids: Solution, diffusion, bubbles and surface effects, with applications to natural samples. *Geochim. Cosmochim. Acta* **51**, 1549–1560 (1987).
42. S. Lorenzetti, H. Busemann, O. Eugster, Regolith history of lunar meteorites. *Meteorit. Planet. Sci.* **40**, 315–327 (2005).
43. C. Thalmann, O. Eugster, G. F. Herzog, S. Xue, J. Klein, U. Krähenbühl, S. Vogt, History of lunar meteorites Queen Alexandra Range 93069, Asuka 881757, and Yamato 793169 based on noble gas isotopic abundances, radionuclide concentrations, and chemical composition. *Meteorit. Planet. Sci.* **31**, 857–868 (1996).
44. J. M. D. Day, L. A. Taylor, C. Floss, A. D. Patchen, D. W. Schnare, D. G. Pearson, Comparative petrology, geochemistry, and petrogenesis of evolved, low-Ti lunar mare basalt meteorites from the LaPaz Icefield, Antarctica. *Geochim. Cosmochim. Acta* **70**, 1581–1600 (2006).
45. T. Arai, B. R. Hawke, T. A. Giguere, K. Misawa, M. Miyamoto, H. Kojima, Antarctic lunar meteorites Yamato-793169, Asuka-881757, MIL 05035, and MET 01210 (YAMM): Launch pairing and possible cryptomare origin. *Geochim. Cosmochim. Acta* **74**, 2231–2248 (2010).
46. L. E. Borg, A. M. Gaffney, C. K. Shearer, D. J. DePaolo, I. D. Hutcheon, T. L. Owens, E. Ramon, G. Brennecka, Mechanisms for incompatible-element enrichment on the Moon deduced from the lunar basaltic meteorite Northwest Africa 032. *Geochim. Cosmochim. Acta* **73**, 3963–3980 (2009).

47. P. H. Warren, G. W. Kallemeyn, Geochemical investigations of two lunar mare meteorites: Yamato-793169 and Asuka-881757. *Proc. NIPR Symp. Antarct. Meteorit.* **6**, 35–57 (1993).
48. K. L. Robinson, J. J. Barnes, K. Nagashima, A. Thomen, I. A. Franchi, G. R. Huss, M. Anand, G. J. Taylor, Water in evolved lunar rocks: Evidence for multiple reservoirs. *Geochim. Cosmochim. Acta* **188**, 244–260 (2016).
49. J. Geiss, G. Gloeckler, Abundances of deuterium and helium-3 in the protosolar cloud. *Space Sci. Rev.* **84**, 239–250 (1998).
50. L. J. Hallis, G. R. Huss, K. Nagashima, G. J. Taylor, S. A. Halldórsson, D. R. Hilton, M. J. Mottl, K. J. Meech, Evidence for primordial water in Earth's deep mantle. *Science* **350**, 795–797 (2015).
51. F. M. McCubbin, K. E. Vander Kaaden, R. Tartése, R. L. Klima, Y. Liu, J. Mortimer, J. J. Barnes, C. K. Shearer, A. H. Treiman, D. J. Lawrence, S. M. Elardo, D. M. Hurley, J. W. Boyce, M. Anand, Magmatic volatiles (H, C, N, F, S, Cl) in the lunar mantle, crust, and regolith: Abundances, distributions, processes, and reservoirs. *Am. Min.* **100**, 1668–1707 (2015).
52. J. P. Greenwood, S. Itoh, N. Sakamoto, P. Warren, L. Taylor, H. Yurimoto, Hydrogen isotope ratios in lunar rocks indicate delivery of cometary water to the Moon. *Nat. Geosci.* **4**, 79–82 (2011).
53. L. Piani, Y. Marrocchi, T. Rigaudier, L. G. Vacher, D. Thomassin, B. Marty, Earth's water may have been inherited from material similar to enstatite chondrite meteorites. *Science* **369**, 1110–1113 (2020).
54. U. Ott, Planetary and pre-solar noble gases in meteorites. *Geochem.* **74**, 519–544 (2014).
55. B. Marty, R. L. Palma, R. O. Pepin, L. Zimmermann, D. J. Schlutter, P. G. Burnard, A. J. Westphal, Helium and neon abundances and compositions in cometary matter. *Science* **319**, 75–78 (2008).
56. J. M. D. Day, D. G. Pearson, L. A. Taylor, ^{187}Re-^{187}Os isotope disturbance in LaPaz mare basalt meteorites, in *Proceedings of the 36th Lunar Planetary Science Conference* (Lunar and Planetary Institute, 2005), abstract 1424.
57. R. M. G. Armytage, R. B. Georg, H. M. Williams, A. N. Halliday, Silicon isotopes in lunar rocks: Implications for the Moon's formation and the early history of the Earth. *Geochim. Cosmochim. Acta* **77**, 504–514 (2012).
58. J. Zhang, N. Dauphas, A. M. Davis, I. Leya, A. Fedkin, The proto-Earth as a significant source of lunar material. *Nat. Geosci.* **5**, 251–255 (2012).
59. C. D. Williams, S. Mukhopadhyay, Capture of nebular gases during Earth's accretion is preserved in deep-mantle neon. *Nature* **565**, 78–81 (2019).
60. M. W. Broadley, P. H. Barry, D. V. Bekaert, D. J. Byrne, A. Caracausi, C. J. Ballentine, B. Marty, Identification of chondritic krypton and xenon in Yellowstone gases and the timing of terrestrial volatile accretion. *Proc. Natl. Acad. Sci. U.S.A.* **117**, 13997–14004 (2020).
61. S. Péron, S. Mukhopadhyay, M. D. Kurz, D. W. Graham, Deep-mantle krypton reveals Earth's early accretion of carbonaceous matter. *Nature* **600**, 462–467 (2021).
62. R. Yokochi, B. Marty, A determination of the neon isotopic composition of the deep mantle. *Earth Planet. Sci. Lett.* **225**, 77–88 (2004).
63. S. Mukhopadhyay, Early differentiation and volatile accretion recorded in deep-mantle neon and xenon. *Nature* **486**, 101–104 (2012).
64. M. Nakajima, D. J. Stevenson, Inefficient volatile loss from the Moon-forming disk: Reconciling the giant impact hypothesis and a wet Moon. *Earth Planet. Sci. Lett.* **487**, 117–126 (2018).
65. P. H. Warren, J. T. Wasson, The origin of KREEP. *Rev. Geophys.* **17**, 73–88 (1979).
66. M. E. I. Riebe, K. C. Welten, M. M. M. Meier, R. Wieler, M. I. F. Barth, D. Ward, M. Laubenstein, A. Bischoff, M. W. Caffee, K. Nishiizumi, H. Busemann, Cosmic-ray exposure ages of six chondritic Almahata Sitta fragments. *Meteorit. Planet. Sci.* **52**, 2353–2374 (2017).
67. P. R. Heck, K. K. Marhas, P. Hoppe, R. Gallino, H. Baur, R. Wieler, Presolar He and Ne isotopes in single circumstellar SiC grains. *Astrophys. J.* **656**, 1208–1222 (2007).
68. H. Baur, A noble gas mass spectrometer compressor source with two orders of magnitude improvement in sensitivity. *Eos. Trans. AGU* **46**, F1118 (1999).
69. A. Meshik, C. Hohenberg, O. Pravdivtseva, D. Burnett, Heavy noble gases in solar wind delivered by Genesis mission. *Geochim. Cosmochim. Acta* **127**, 326–347 (2014).
70. P. Eberhardt, O. Eugster, K. Marti, Notizen: A redetermination of the isotopic composition of atmospheric neon. *Z. Naturforsch. A* **20**, 623–624 (1965).
71. J.-Y. Lee, K. Marti, J. P. Severinghaus, K. Kawamura, H.-S. Yoo, J. B. Lee, J. S. Kim, A redetermination of the isotopic abundances of atmospheric Ar. *Geochim. Cosmochim. Acta* **70**, 4507–4512 (2006).
72. J. R. Basford, J. C. Dragon, R. O. Pepin, M. R. Coscio Jr., V. R. Murthy, Krypton and xenon in lunar fines, in *Proceedings of the 4th Lunar Conference* (Lunar and Planetary Institute, 1973), pp. 1915–1955.
73. B. A. Mamyrin, G. S. Anufriev, I. L. Kamenskii, I. N. Tolstikhin, Determination of the isotopic composition of atmospheric helium. *Geochem. Int.* **7**, 498–505 (1970).
74. H. Hintenberger, H. W. Weber, Trapped rare gases in lunar fines and breccias, in *Proceedings of the 4th Lunar Science Conference* (Lunar and Planetary Institute, 1973), pp. 2003–2019.
75. P. Eberhardt, O. Eugster, J. Geiss, N. Groegler, S. Guggisberg, M. Mörgeli, Noble gases in the Apollo 16 special soils from the East-West split and the permanently shadowed area, in *Proceedings of the 7th Lunar Science Conference* (Pergamon Press Inc., 1976), pp. 563–585.
76. T. Mijajlovic, X. Xue, E. Walton, A revised shock history for the youngest unbrecciated lunar basalt–Northwest Africa 032 and paired meteorites. *Meteorit. Planet. Sci.* **55**, 2267–2286 (2020).
77. J. Eikenberg, P. Signer, R. Wieler, U-Xe, U-Kr, and U-Pb systematics for dating uranium minerals and investigations of the production of nucleogenic neon and argon. *Geochim. Cosmochim. Acta* **57**, 1053–1069 (1993).
78. I. Leya, J. Masarik, Cosmogenic nuclides in stony meteorites revisited. *Meteorit. Planet. Sci.* **44**, 1061–1086 (2009).
79. K. H. Joy, S. S. Russell, A. T. Kearsley, I. A. Crawford, Lunar mare basaltic meteorites—LAP 02205, LAP 02224 and LAP 02226. *Geophys. Res. Abs.* **7**, A04088 (2005).
80. K. Righter, S. J. Collins, A. D. Brandon, Mineralogy and petrology of the LaPaz Icefield lunar mare basaltic meteorites. *Meteorit. Planet. Sci.* **40**, 1703–1722 (2005).
81. R. A. Zeigler, R. L. Korotev, B. L. Jolliff, L. A. Haskin, Petrography and geochemistry of the LaPaz Icefield basaltic lunar meteorite and source crater pairing with Northwest Africa 032. *Meteorit. Planet. Sci.* **40**, 1073–1101 (2005).
82. K. Thiel, W. Herr, J. Becker, Uranium distribution in basalt fragments of five lunar samples. *Earth Planet. Sci. Lett.* **16**, 31–44 (1972).
83. J. Funkhouser, E. Jessberger, O. Müller, J. Zähringer, Active and inert gases in Apollo 12 and Apollo 11 samples released by crushing at room temperature and by heating at low temperatures, in *Proceedings of the 2nd Lunar Science Conference* (MIT Press, 1971), pp. 1381–1396.
84. O. Eugster, N. Grögler, M. D. Mendia, P. Eberhardt, J. Geiss, Trapped solar wind noble gases and exposure age of Luna 16 lunar fines. *Geochim. Cosmochim. Acta* **37**, 1991–2003 (1973).
85. S. P. Schwenzer, J. Fritz, D. Stöffler, M. Trieloff, M. Amini, A. Greshake, S. Herrmann, K. Herwig, K. P. Jochum, R. K. Mohapatra, B. Stoll, U. Ott, Helium loss from Martian meteorites mainly induced by shock metamorphism: Evidence from new data and a literature compilation. *Meteorit. Planet. Sci.* **43**, 1841–1859 (2008).
86. S. Regnier, C. M. Hohenberg, K. Marti, R. C. Reedy, Predicted versus observed cosmic-ray-produced noble gases in lunar samples: Improved Kr production ratios, in *Proceedings of the 10th Lunar Planetary Science Conference* (Lunar and Planetary Institute, 1979), pp. 1565–1586.
87. N. Bhandari, D. Lal, R. S. Rajan, J. R. Arnold, K. Marti, C. B. Moore, Atmospheric ablation in meteorites: A study based on cosmic ray tracks and neon isotopes. *Nucl. Tracks* **4**, 213–262 (1980).
88. V. A. Alexeev, Meteorite ablation evaluated from data on the distribution of cosmogenic neon isotopes. *Solar Syst. Res.* **37**, 207–217 (2003).
89. J.-P. Benkert, H. Baur, P. Signer, R. Wieler, He, Ne, and Ar from the solar wind and solar energetic particles in lunar ilmenites and pyroxenes. *J. Geophys. Res.* **98**, 13147–13162 (1993).

Acknowledgments: We thank the NASA Antarctic MWG for the allocation of sample splits of the six Antarctic LAP meteorites and loan of thin sections of the LAP 02205, 02224, 02226, and 02436 meteorites. R. Wieler and M. Schönbächler are acknowledged for discussions that improved the manuscript. **Funding:** This work was supported by Swiss National Science Foundation grants 200021_163098 and 200020_182649 (to H.B., supporting P.W.) and has been carried out within the framework of the NCCR PlanetS supported by the Swiss NSF under grants 51NF40_182901 and 51NF40_205606 (to H.B., supporting M.E.I.R.). **Author contributions:** Conceptualization: P.W. and H.B. Sample handling and mineral separation: P.W. Mass spectrometric analyses and data reduction: P.W. Maintenance of all mass spectrometers: C.M. Data interpretation and major conclusions: P.W., H.B., and M.E.I.R. Writing—original draft: P.W. Writing—review and editing: P.W., H.B., M.E.I.R., and C.M. **Competing interests:** The authors declare that they have no competing interests. **Data and materials availability:** All data needed to evaluate the conclusions in the paper are present in the paper and/or the Supplementary Materials.

Submitted 16 July 2021
Accepted 29 June 2022
Published 10 August 2022
10.1126/sciadv.abl4920